

COOLING OF AN ISOTHERMAL PLATE BY A CONFINED TWO-DIMENSIONAL AIR JET

Márcio Antonio Bazani - bazani@fem.unicamp.br

Carlos A.C. Altemani - altemani@fem.unicamp.br

Universidade Estadual de Campinas - FEM - Departamento de Energia

Caixa Postal 6122 - CEP 13.083-970 - Campinas - SP - Brazil

***Abstract.** Atmospheric air is the most convenient fluid for the cooling of electronic equipment but, due to its thermal properties, enhanced convective heat transfer techniques are usually required for the proper thermal design. One possibility consists of impinging turbulent air jets on the components' surfaces, usually within confined spaces. The purpose of this paper is to present numerical results associated to the convective cooling of a heated plate by a two-dimensional turbulent air jet. The air jet issues from a slot on the confinement plate, directed normal to the parallel impingement plate. It spreads symmetrically, confined in the space between the two parallel plates. The high-Reynolds $k-\epsilon$ turbulence model with wall functions was used for the numerical simulations of the flow and heat transfer. The effects of the plates' distance, the slot width and the jet Reynolds number on the convective heat transfer were considered in the analysis. Comparisons were made with numerical and experimental results from the literature. A sensitivity analysis was carried out for distinct parameters of the adopted turbulence model.*

Keywords: confined 2D jet, $k-\epsilon$ turbulence model, numerical results, heat transfer comparisons.

1. INTRODUCTION

Atmospheric air is the most convenient coolant fluid for electronic equipment but, due to its thermal properties, the thermal design usually requires the use of a heat transfer augmentation technique. Jets have been used in several heat and mass transfer engineering applications for many years, e.g., for the drying of paper and textiles and for the annealing of plastics and metals, giving rise to many experimental data correlations reviewed by Martin (1977). Other more recent applications include turbine-blade cooling (Florschuetz et al., 1984) and the thermal management of electronics (Bergles and Bar-Cohen, 1990). In this case, the desired thermal control must be met taking into account several engineering constraints: the available fluid flow rate, the maximum pressure drop, the pumping power and other, like the manufacturing and maintenance considerations (Maddox and Bar-Cohen, 1994). There are several experimental data for two-dimensional slot air jets, mostly for unconfined jets (Gardon and Akfirat, 1966), but also for confined jets (Ichimiya and Hosaka, 1992). Turbulence models have been applied to the flow and thermal predictions of impinging jets since the pioneering work of Wolfshtein (1969). A review of distinct turbulence models applied to jets' simulations was presented by Polat et al. (1989). The most extensively used turbulence model in the literature is the $k-\epsilon$ two-equation model (Launder and Spalding, 1974). Several modifications to the original model were made: the low-Reynolds models (Lam and Bremhorst, 1981), the two-layer models (Chieng and Launder, 1980), the two-scale models (Kim and Chen, 1989), and the

renormalization group - RNG models (Yakhot and Orszag, 1986). Usually the experimental heat transfer coefficient at the stagnation region of turbulent jets impinging on a flat plate are underpredicted by the traditional k- ϵ model and overpredicted by the modified k- ϵ models. Several reports illustrate these trends: Amano and Sugiyama, 1985, Polat et al., 1990, Chen, 1995, Hosseinalipour and Mujumdar, 1995, Seyedein et al., 1994 and Morris et al., 1996. Two points may be concluded from the literature survey. First, many researchers have adopted the k- ϵ turbulence model for several years and its capabilities and limitations to predict the turbulent jet flow and heat transfer are well documented - it is reasonably accurate and economic from the computational point of view. Second, the single turbulent jet impinging on a flat plate, despite its apparent simplicity, has been a test for turbulence models for many years and still deserves attention and further study.

The present work was undertaken as a first step to an application of turbulent air jets to the cooling of electronic components. A high Reynolds number k- ϵ turbulence model was employed in conjunction with near-wall functions used in the place of wall boundary conditions. The flow and heat transfer characteristics of a confined turbulent two-dimensional air jet impinging on a flat plate were predicted solving the conservation and the turbulence model equations with a finite volumes algorithm. The results obtained were compared with numerical and experimental data from the literature.

2. ANALYSIS

The two-dimensional air jet considered in this work is indicated in Fig.1. The jet issues with a uniform velocity V_{in} and temperature T_{in} from the slot of width \underline{W} on the confinement plate. It is directed to the parallel impingement plate, at a distance \underline{H} from the jet entrance. The y-axis is a symmetry line for the flow and heat transfer. The calculation domain extended from the symmetry line to $(L/2)$ in the x-direction, occupying the space between both plates. The impingement plate was isothermal at T_w , while the confinement plate was adiabatic.

2.1 Mathematical model

The flow and heat transfer characteristics were obtained from the numerical solution of the conservation and the turbulence model equations. The air flow was turbulent from the entrance and the time averaged or the Reynolds form of the transport equations was utilized. Considering an incompressible steady turbulent flow, these equations were the following, using index notation. The capital letters \underline{U}_i and \underline{T} indicate respectively the time averaged velocity components and temperature while the small letters \underline{u}_i and \underline{t} represent their instantaneous fluctuations.

Continuity:

$$\frac{\partial U_i}{\partial x_i} = 0 \quad (1)$$

Momentum:

$$U_j \frac{\partial U_i}{\partial x_j} = -\frac{\partial P}{\partial x_i} + \frac{\partial}{\partial x_j} \left[\mu \left(\frac{\partial U_i}{\partial x_j} + \frac{\partial U_j}{\partial x_i} \right) - \rho \overline{u_i u_j} \right] \quad (2)$$

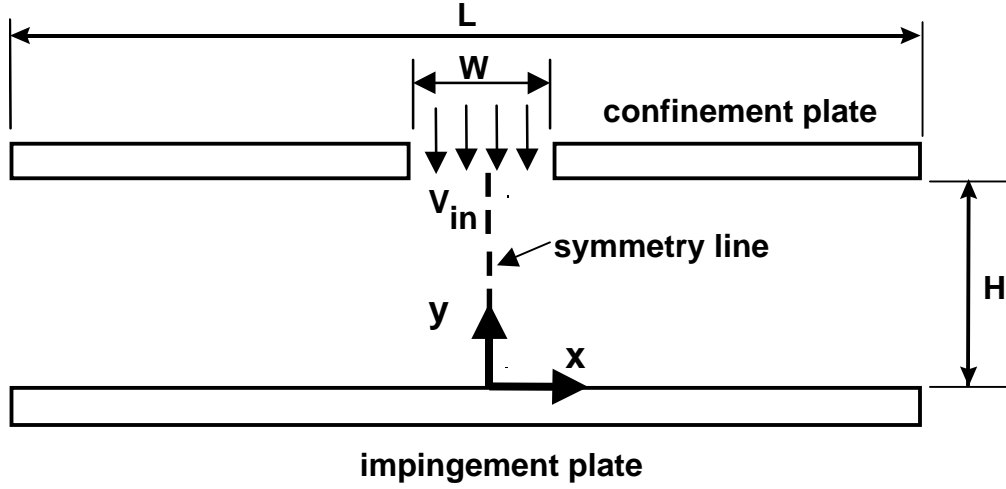


Fig. 1 - Domain configuration and notation

Energy:

$$\rho U_j \frac{\partial T}{\partial x_j} = \frac{\partial}{\partial x_j} \left[\frac{\mu}{\text{Pr}} \frac{\partial T}{\partial x_j} - \overline{\rho u_j t} \right] \quad (3)$$

The terms $(-\overline{\rho u_i u_j})$ and $(-\overline{\rho u_j t})$ in the momentum and energy equations represent respectively the Reynolds stresses and the turbulent heat fluxes. Since they constitute new flow variables, they were related to the average velocities and temperature distributions using the concepts of the Boussinesq turbulent viscosity μ_t and the turbulent Prandtl number σ_T :

$$-\overline{\rho u_i u_j} = \mu_t \left(\frac{\partial U_i}{\partial x_j} + \frac{\partial U_j}{\partial x_i} \right) \quad \text{and} \quad -\overline{\rho u_j t} = \frac{\mu_t}{\sigma_T} \frac{\partial T}{\partial x_j} \quad (4)$$

Rather than being a fluid property, the turbulent viscosity μ_t depends on the local flow conditions. Several relationships of μ_t to the mean flow variables can be found in the literature, characterizing distinct turbulence models. The model used in this work was the high-Re version of the two-equation k - ε turbulence model, developed by Launder and Spalding (1974). This is a well-established model, validated by many works in the literature and well suited for recirculating confined flows, where the convection and diffusion of the turbulent kinetic energy must be taken into account.

In this model the turbulent viscosity is related to the turbulent kinetic energy \underline{k} and to its dissipation rate $\underline{\varepsilon}$:

$$\mu_t = \rho C_\mu \frac{k^2}{\varepsilon}, \quad \text{where} \quad k = \frac{1}{2} (\overline{u^2} + \overline{v^2}) \quad (5)$$

and C_μ is a constant of the model.

The local values of \underline{k} and $\underline{\varepsilon}$ are obtained from the solution of two additional transport equations:

$$\frac{\partial}{\partial x_j} (\rho U_j k) = \frac{\partial}{\partial x_j} \left(\frac{\mu_t}{\sigma_k} \frac{\partial k}{\partial x_j} \right) + (G - \rho \epsilon) \quad (6)$$

and

$$\frac{\partial}{\partial x_j} (\rho U_j \epsilon) = \frac{\partial}{\partial x_j} \left(\frac{\mu_t}{\sigma_\epsilon} \frac{\partial \epsilon}{\partial x_j} \right) + (C_{1\epsilon} G - C_{2\epsilon} \rho \epsilon) \frac{\epsilon}{k} \quad (7)$$

The term G appearing in both eq. (6) and (7) is the rate of production of turbulent kinetic energy, modeled by

$$G = \mu_t \left(\frac{\partial U_i}{\partial x_j} + \frac{\partial U_j}{\partial x_i} \right) \frac{\partial U_i}{\partial x_j} \quad (8)$$

The constants appearing in eq. (5) - (7) are characteristic of the turbulence model and their values were (Launder and Spalding, 1974): $C_\mu = 0.09$ - $C_{1\epsilon} = 1.43$ - $C_{2\epsilon} = 1.92$ - $\sigma_k = 1.0$ and $\sigma_\epsilon = 1.3$. The standard value $\sigma_T = 0.9$ was assigned to the turbulent Prandtl number appearing in eq. (4).

Boundary conditions. Due to the symmetry indicated in Fig. 1, the conservation equations (1) to (3) and the turbulence model equations (6) and (7) were solved for only one side of the flow domain. Their boundary conditions were stated as follows.

At the jet entrance the normal velocity and the temperature were uniform:

$$0 \leq x \leq \frac{W}{2} \quad \text{and} \quad y = H : \quad u = 0, \quad v = V_{in}, \quad T = T_{in} \quad (9)$$

It is noticed that $(V_{in} \cdot W / \nu)$ defined the jet Reynolds number.

The turbulence kinetic energy and the rate of its dissipation at the entrance were specified as follows:

$$k_{in} = I^2 V_{in}^2 \quad \text{and} \quad \epsilon_{in} = \frac{C_\mu k_{in}^{3/2}}{AW} \quad (10)$$

where \underline{A} is a constant. Since distinct values of the turbulence intensity \underline{I} and the constant \underline{A} were found in the literature, a sensitivity analysis was performed to investigate their effects on the numerical results, to be presented later.

At the outflow boundary, the x-derivatives of the v-velocity, the temperature and the variables k and ϵ of the turbulence model were set equal to zero. The u-velocity was obtained imposing mass conservation over the computational domain.

At the symmetry line ($x = 0$) the u-velocity and the x-derivative of the remaining variables (v, T, k, ϵ) were set equal to zero.

The solid walls ($y = 0$ and $y = H$) were impermeable, so that the v-velocity was set equal to zero. The no slip condition was adopted for the u-velocity and according to the high-Re turbulence model, there was no need to integrate the equations over the near-wall region. Instead, the wall functions method suggested by Launder and Spalding (1974) was employed. The near-wall u-velocity was modeled as

$$y^+ > 11.5: \quad U^+ = \frac{1}{\kappa} \ln(Ey^+) \quad (11a)$$

$$y^+ \leq 11.5: \quad U^+ = y^+ \quad (11b)$$

In this equation, κ is the von Karman's constant (0.4) and E is an integration constant, assumed equal to 9 for smooth walls. The dimensionless variables U^+ and y^+ are defined by

$$U^+ = \frac{U}{U^*} \quad \text{and} \quad y^+ = \frac{U^* y}{\nu} \quad (12)$$

where the velocity scale U^* is given by $U^* = \sqrt{\frac{\tau_w}{\rho}}$.

The impingement plate was isothermal at T_w and the confinement plate was adiabatic. The near-wall temperature T was also treated by the wall-function method. The resulting local shear stress and heat flux at the impingement plate were expressed by

$$y^+ > 11.5: \quad \tau_w(x) = \frac{\kappa \rho c_p^{1/4} k^{1/2} U}{\ln(Ey^+)} \quad \text{and} \quad q_w''(x) = \frac{\rho c_p c_p^{1/4} k^{1/2} (T_w - T)}{\sigma_T (U^+ + P^+)} \quad (13a)$$

$$y^+ \leq 11.5: \quad \tau_w(x) = \mu \frac{U}{y} \quad \text{and} \quad q_w''(x) = k \frac{T_w - T}{y} \quad (13b)$$

The P^+ -function in eq. (13a) depends on the laminar to turbulent Prandtl numbers ratio:

$$P^+ = 9 \left(\frac{\sigma}{\sigma_T} - 1 \right) \left(\frac{\sigma_T}{\sigma} \right)^{1/4} \quad (14)$$

The heat flux evaluated by eq. (13) was employed to obtain a local Nusselt number:

$$Nu(x) = \frac{q_w''(x)W}{k(T_w - T_{in})} \quad (15)$$

The diffusion of turbulent kinetic energy was set equal to zero at the walls:

$$y = 0 \quad \text{and} \quad y = H: \quad \frac{\partial k}{\partial y} = 0 \quad (16)$$

The dissipation rate of turbulent kinetic energy tends to infinity at the wall, but a finite value was set at a near-wall position, according to

$$\varepsilon_P = \frac{c_\mu^{3/4} k_P^{3/2}}{\kappa y} \quad (17)$$

2.2 Numerical solution

The dimensional conservation and turbulence model equations were solved numerically, employing the control volumes method. The only fluid considered was air, with an inlet temperature equal to 290 K. The impingement wall temperature was 310 K. All the equations were discretized, resulting in a system of linearized algebraic equations for the nodal points of the solution domain. Along the y-direction, the grid spacing was smaller near the walls and increased according to a geometric progression to the central region. Along the x-direction, the grid spacing was uniform under the jet and then it increased also according to a geometric progression to the outflow boundary. The progression ratio was obtained for each case considering the height H, the length L and the number of grid points in each direction - typical values ranging from 1.05 to 1.15.

The algebraic system of equations was solved iteratively until convergence, employing the line-by-line method. In each iteration, first the continuity and momentum equations were solved employing the SIMPLE algorithm with the power-law scheme (Patankar, 1980). Next, the energy and both turbulence model equations were solved. At the end of each iteration, the partial solution obtained was used to calculate the coefficients and the source terms of the algebraic equations for the next iteration. The convergence was attained with relaxation of the variables in the numerical solution. The factors employed for the u and v velocity components and the pressure were respectively 0.5, 0.5, and 0.6. For the k and ε equations, they were equal to 0.4 and the turbulence viscosity μ_t was under-relaxed with the factor 0.5. The criterion for convergence was that the maximum mass residual for any control volume of the domain was smaller than 10^{-7} . This residual was attained in about 1000 iterations of the computer program for the cases investigated, using about 5 minutes of a Sun Sparc 10 workstation.

3. RESULTS

The effects of the grid size and the position of the near-wall node are indicated in Fig. 2 for $Re = 20,000$, the ratio $(H/W) = 8$ and the turbulence intensity $I = 1$ per cent. For the four distinct grids indicated in Fig. 2a, the Nu distributions along the impingement plate remained within 3 per cent of each other, although the number of grid points changed from 600 to 2,400. Thus, the 30x30 grid was enough to obtain the results for this configuration. The results to be presented next will however have distinct grids because the comparisons with numerical data from the literature were made employing the same number of grid points.

The data presented in Fig. 2b were obtained with a grid of 30x30 and indicated that the stagnation Nu number changed less than 2 per cent when the y^+ value of the near-wall grid point varied in the range from 180 to 580. Thus, the universal velocity and temperature profiles used in the turbulence model are adequate to obtain consistent results for a range of y^+ values.

The effects of the turbulence kinetic energy and the rate of its dissipation at the jet entrance on the Nu distribution were investigated through the values of the turbulence intensity \underline{I} and the constant \underline{A} defined in eq. (10). The results are indicated in Fig. 3 for the same case: $Re = 20,000$ and the ratio $(H/W) = 8$. The Nu distributions of Fig. 3a indicate the results for three values of the turbulence intensity I equal to 1, 5 and 10 per cent, with a grid of 60x40 control

volumes. For this range of 10 to 1 of the turbulence intensity, the largest effect on the local Nu is limited to 5 per cent at the stagnation point and to smaller variations at the downstream positions. The effect of the constant A on the Nu distribution at the impingement plate is indicated in Fig. 3b, for the same Re and (H/W) of the previous figures, with I = 1 per cent at the jet entrance and a grid of 30x30. The values of the constant A are those usually found in the literature and the results indicated a negligible effect of A on the local Nu distribution.

The isotherms and the streamlines presented in Fig. 4 correspond to Re = 9,900 and the ratio (H/W) = 2.5, with I = 1 per cent and A = 0.05, employing a 32x32 grid. For the domain length equal to 25 times the slot width W, the recirculation zone of the confined jet is contained within the solution domain. The recirculation zone increased with the Reynolds number and the aspect ratio (H/W), so that the ratio (L/2W), characteristic of the solution domain length, should be verified in order to satisfy exactly the stated outflow boundary conditions. The isotherms indicate that, as expected from the turbulent confined jet flow, the temperature gradients are concentrated very near the impingement surface.

Other typical mean flow properties, such as the inlet velocity decay along the symmetry line and the pressure at the impingement plate, are indicated in Fig. 5. The jet velocity decay curves shown in Fig. 5a indicate that the presence of the impingement plate is felt at distances closer to the jet inlet ($y = H$) as the ratio (H/W) decreases. The jet potential core region is considered the distance from the jet inlet where the velocity at the symmetry line decreases to 95 per cent of V_{in} . The curve for (H/W) = 7.5 indicates a value equal to 5.47 slot widths (W) for this condition. Corresponding values found in the literature (Seyedein et al., 1994) indicate, for the same conditions, a range from 5.1 to 5.9, depending on the turbulence model used, while an experimental value was equal to 5.2. The static pressure distribution along the impingement plate was expressed in dimensionless form by

$$DP(x) = \frac{P_w(x) - P_w(L)}{P_w(0) - P_w(L)} \quad (18)$$

where the subscript w indicates the impingement wall. Typically, the confined jet static pressure distribution at the impingement plate is maximum at the stagnation line, attains a minimum at the end of the so-called stagnation region, and then increases monotonically to the outflow boundary. In Fig. 5b, the negative values of the dimensionless pressure reflect the described behavior. These results were obtained with a 32x32 grid.

The Nu predictions are more sensitive to the turbulence model near-wall functions than the mean flow properties. In Fig. 6, the Nu distributions obtained in this work for two pairs of Re and (H/W) are compared with numerical and experimental data from the literature. The results were obtained with the same number of grid points (25x15) used by Polat et al. (1990) for the high-Re k-ε model. The current results compare much better with the experiments at the stagnation region, where usually the predictions are more difficult. They also do not show a false second peak as many other predictions do for the relatively large values of (H/W) in Fig.6. Concerning the experimental data, only those of Cadek, 1968, were obtained for a confined jet - the others were obtained for unconfined slot jets.

4. CONCLUSIONS

The flow and heat transfer characteristics of turbulent confined slot jets were obtained numerically employing a high Re k-ε turbulence model. The conservation and the model equations were solved iteratively with the SIMPLE algorithm, for distinct values of the geometric ratio (H/W) and the jet Reynolds number, considering air as the working fluid.

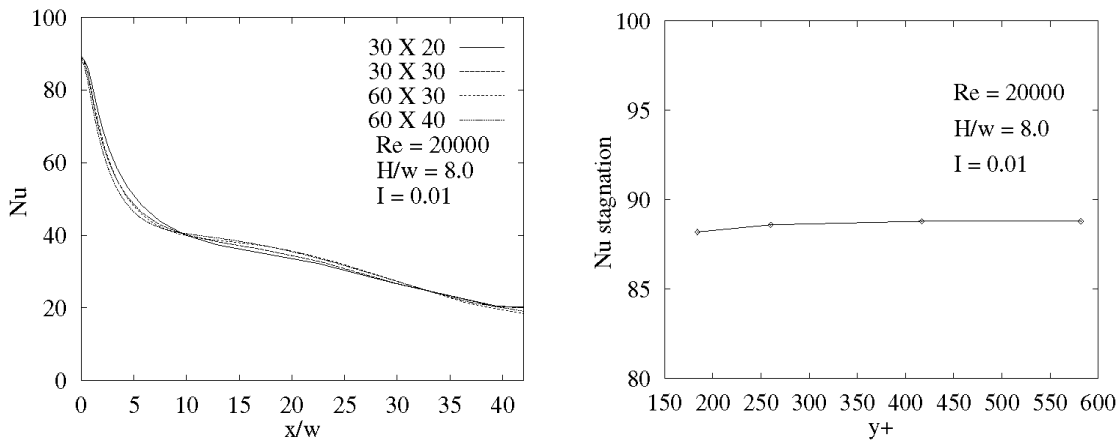


Fig. 2 (a) - Effects of (a) the grid size and (b) the position y^+ of the near-wall grid.

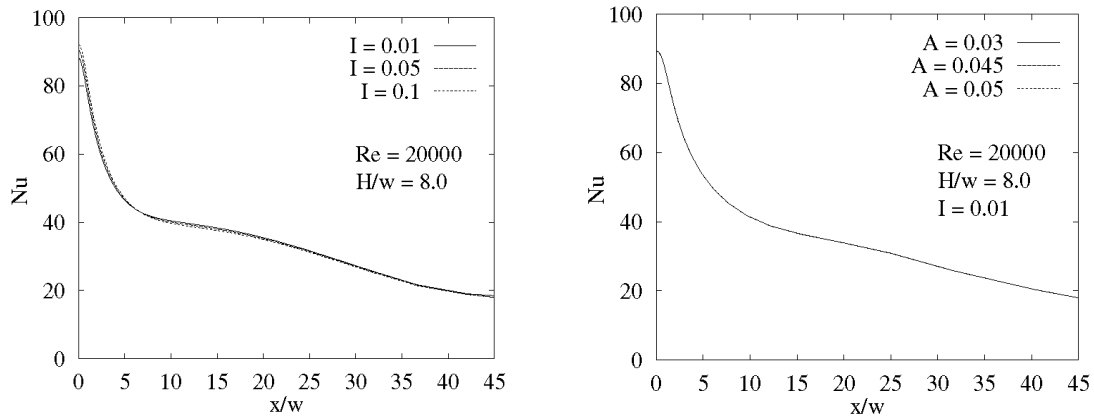


Fig. 3 Effects of (a) the turbulence intensity and (b) the dissipation rate at the jet entrance.

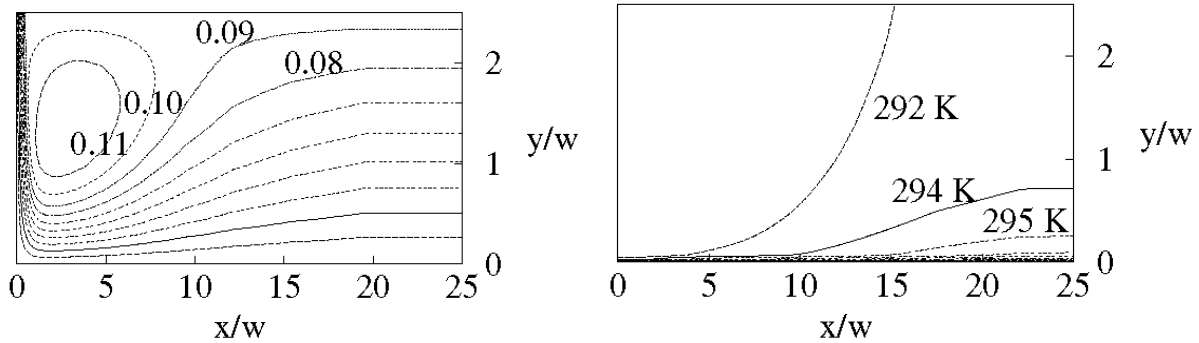


Fig. 4 Streamlines (a) and isotherms (b) for $Re = 9,900$ and $(H/W) = 2.5$.

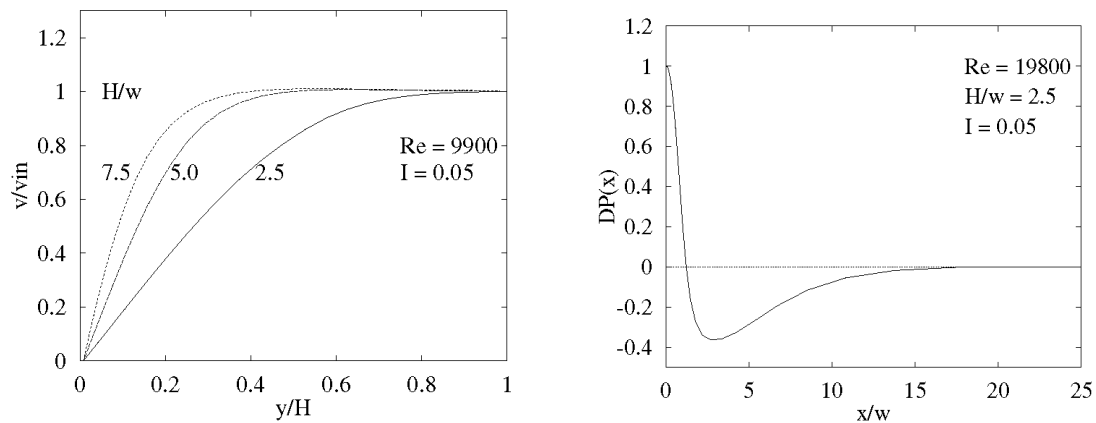


Fig.5 Jet velocity decay at $x = 0$ (a) and pressure distribution at the impingement plate (b)

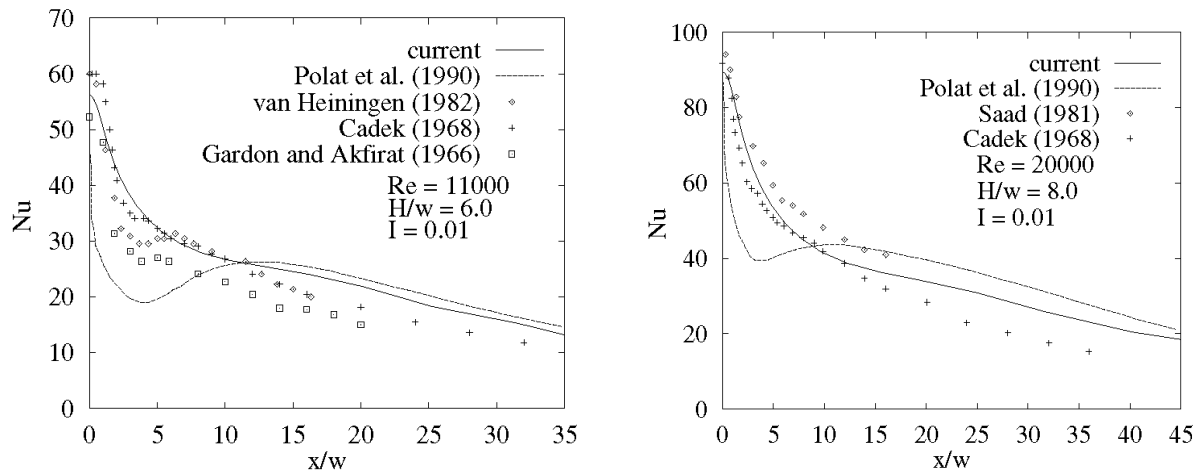


Fig. 6 Nusselt predictions compared with data from the literature

The selection of the wall functions used in the turbulence model may influence the numerical results, notably the heat transfer predictions at the stagnation region. Compared to other numerical predictions using the same turbulence model, but with distinct wall functions, the present work showed better agreement with experimental data.

The decay of the jet inlet velocity at the symmetry line also compared favorably with data from the literature. The pressure distributions along the impingement plate, the streamlines and the isotherms of the confined jet flow were all obtained with physical realism, comparable to results presented in the literature.

A sensitivity analysis of the inlet values of k and ϵ on the Nusselt distribution indicated that their influence is small (less than 5 per cent) within the range of values usually found in the literature.

The turbulent slot jet problem, despite its simple configuration, remains a challenge for flow and heat transfer modeling. The high-Re k - ϵ is probably the most used and tested turbulence model, so that its limitations and capabilities to predict recirculating flows are well documented in the literature. The current procedure will be applied next to predict the cooling of discrete flush mounted heaters on the impingement plate.

Acknowledgments

The support of FAPESP and the scholarship of CNPq to the first author are deeply acknowledged.

REFERENCES

- Amano, R. S., and Sugiyama, S., 1985, An Investigation on Turbulent Heat Transfer of an Axisymmetric Jet Impinging on a Flat Plate, *Bulletin of JSME*, vol. 28, pp. 74-79.
- Bergles, A. E., and Bar-Cohen, A., 1990, Direct Liquid Cooling of Microelectronic Components, *Advances in Thermal Modeling of Electronic Components and Systems* - vol. 2, ASME Press, pp. 233-342.
- Cadek, F.F., 1968, A Fundamental Investigation of Jet Impingement Heat Transfer, Ph.D. Thesis, University of Cincinnati, OH, EUA.

- Chen, Q., 1995, Comparison of Different k - ϵ Models for Indoor Air Flow Computations, Numerical Heat Transfer, Part B, vol. 28, pp. 353-369.
- Chieng, C. C., and Launder, B. E., 1980, On the Calculation of Turbulent Heat Transport Downstream From an Abrupt Pipe Expansion, Numerical Heat Transfer, vol. 3, pp. 189-207.
- Florschuetz, L. W., Metzger, D. E., and Su, C. C., 1984, Heat Transfer Characteristics for Jet Array Impingement with Initial Crossflow, J. of Heat Transfer, vol.106, pp. 34-41.
- Gardon, R., and Akfirat, J. C., 1966, Heat Transfer Characteristics of Impinging Two Dimensional Air Jets, J. of Heat Transfer, vol. 88, pp. 101-108.
- Hosseinalipour, S. M., and Mujumdar, A. S., 1995, Comparative Evaluation of Different Turbulence Models for Confined Impinging and Opposing Jets, Numerical Heat Transfer, Part A, vol. 28, pp. 647-666.
- Ichimiya, K., and Hosaka, N., 1992, Experimental Study of Heat Transfer Characteristics due to Confined Impinging Two-Dimensional Jets, Experimental thermal and Fluid Science, vol. 5, pp. 803-807.
- Kim, S. W., and Chen, C. P., 1989, A Multi-Time-Scale Turbulence Model Based on Variable Partitioning of the Turbulent Kinetic Energy Spectrum, Numerical Heat Transfer, Part B, vol. 16, pp. 193-211.
- Lam, C. K. G., and Bremhorst, K., 1981, A Modified Form of the k - ϵ model for Predicting Wall Turbulence, J. Fluids Engineering, vol. 103, pp. 456-460.
- Launder, B. E., and Spalding, D. B., 1974, The Numerical Computation of Turbulent Flows, Computer Methods in Applied Mechanics and Engineering, vol. 3, pp. 269-289.
- Maddox, D. E., and Bar-Cohen, A., 1994, Thermofluid Design of Single-Phase Submerged Jet Impingement Cooling for Electronic Components, J. of Electronic Packaging, vol. 116, pp. 237-240.
- Martin, H., 1977, Heat and Mass Transfer between Impinging Gas Jets and Solid Surfaces, Advances in Heat Transfer, Academic Press, vol. 13, pp. 1-60.
- Morris, G. K., Garimella, S. V., and Amano, R. S., 1996, Prediction of Jet Impingement Heat Transfer Using a Hybrid Wall Treatment with Different Turbulent Prandtl Number Functions, J. of Heat Transfer, vol. 118, pp. 562-569.
- Patankar, S. V., Numerical Heat Transfer and Fluid Flow, Hemisphere Publishing Co., 1980
- Polat, S., Huang, B., Mujumdar, A. S., and Douglas, W. J. M., 1989, Numerical Flow and Heat Transfer Under Impinging Jets: A Review, Annual review of Numerical Fluid Mechanics and Heat Transfer, vol.2, pp. 157-197.
- Polat, S., Mujumdar, A. S., van Heiningen, A. R. P., and Douglas, W. J. M., 1990, Effect of Near-Wall Modeling on Prediction of Impingement Heat Transfer, Drying Technology, vol. 8, pp. 705-730.
- Seyedein, S. H., Hasan, M., and Mujumdar, A. S., 1994, Modelling of a Single Confined Turbulent Slot Jet Impingement Using Various k - ϵ Turbulence Models, Appl. Math. Modelling, vol. 18, pp. 526-537.
- Wolfshtein, M., 1969, Some Solutions of the Plane Turbulent Impinging Jet, J. of Basic Engineering, vol.38, pp.577-612.
- Yakhot, V., and Orszag, S. A., 1986, Renormalization Group Analysis of Turbulence: I. Basic Theory, J. Scientific Computation, vol.1, pp. 1-51.